Limits of calcium isotopes diagenesis in fossil bone and enamel

Pierre-Jean Dodat, Jeremy E. Martin, Sébastien Olive, Auguste Hassler, Emmanuelle Albalat, Jean-Renaud Boisserie, Gildas Merceron, Antoine Souron, Bruno Maureille, Vincent Balter

Limits of calcium isotopes diagenesis in fossil bone and enamel

Pierre-Jean Dodat [1,2], Jeremy E. Martin [1], Sébastien Olive [1,3], Auguste Hassler[1,4,5], Emmanuelle Albalat [1], Jean-Renaud Boisserie [6,7], Gildas Merceron [6], Antoine Souron [2], Bruno Maureille [2], Vincent Balter [1,*]

1 : LGL-TPE, UMR 5276, ENS de Lyon, CNRS, Univ. Lyon 1. 46 Allée d'Italie, 69342 Lyon Cedex 07, France.0

2 : PACEA UMR 5199, Univ. Bordeaux, CNRS, MC, F-33600 Pessac France.

3 : Directorate Earth & Life History, Royal Belgian Institute of Natural Sciences, Rue Vautier 29, 1000 Brussels, Belgium

4 : Present address: Department of Archaeology, University of Aberdeen, Aberdeen, United Kingdom

5 : Present address: Department of Earth and Environmental Sciences, University of Ottawa, Ottawa, ON, Canada.

6 : PALEVOPRIM, UMR 7262, CNRS, Univ. Poitiers, 86073 Poitiers, France

7 : CFEE UAR 3137, CNRS, Ministère de l'Europe et des affaires étrangères, PO BOX 5554 Addis Ababa, Ethiopia

* Corresponding author: vincent.balter@ens-lyon.fr

Abstract

Diagenesis has been recognized for decades to significantly alter the trace elements biogenic signatures in fossil tooth enamel and bone that are routinely used for paleobiological and paleoenvironmental reconstructions. This signature is modified during diagenesis according to a complex continuum between two main processes, addition, and substitution. For an additive-like, or early diagenesis, the trace elements biogenic profiles can be restored by leaching secondary minerals, but this technique is inefficient for a substitutive-like, or extensive diagenesis for which secondary trace elements are incorporated into the biogenic mineral. This scheme is however unclear for Ca, the major cation in tooth enamel and bone hydroxylapatite, which stable isotope composition ($\delta^{44/42}$Ca) also conveys biological and environmental information. We present a suite of leaching experiments for monitoring $\delta^{44/42}$Ca values in artificial and natural fossil enamel and bone from different settings. The results show that enamel $\delta^{44/42}$Ca values are insensitive to an additive-like diagenesis that involves the formation of secondary Ca-carbonate mineral phases, while bone shows a consistent offset toward ^{44}Ca-enriched values, that can be restored to the biogenic baseline by a leaching procedure. In the context of a substitutive-like diagenesis, bone exhibits constant $\delta^{44/42}$Ca values, insensitive to leaching, and shows a REE pattern symptomatic of extensive diagenesis. Such a REE pattern can be observed in fossil enamel for which $\delta^{44/42}$Ca values are still fluctuating and follow a trophic pattern. We conclude that Ca isotopes in fossil enamel are probably not prone to extensive diagenesis and argue that this immunity is due to the very low porosity of enamel that cannot accommodate enough secondary minerals to significantly modify the isotopic composition of the enamel Ca pool.

1. Introduction

Bone, dentin, and enamel are valuable archives for recording information about the life history and environment of fossil and extant vertebrates. The information is embedded as trace elements or isotopic ratios signature during the genesis of the mineralized tissue, a signature that is further obfuscated by diagenesis during fossilization. Regarding trace elements, the comprehension of diagenetic mechanisms has greatly benefited from in-situ laser ablation measurements (Kohn and Moses, 2013; Kral et al., 2022), highlighting the complex interplay of the diffusion, adsorption, and transport reaction processes. However, while sophisticated techniques are now deployed to fully integrate all the hallmarks of diagenesis (Suarez and Kohn, 2020; Weber et al., 2021; Kral et al., 2022), the results still recognize the central importance of porosity which was already suspected in the 2000's (Hedges, 2002; Trueman and Tuross, 2002; Kral et al., 2021). Porosity mediates fluid circulation and secondary mineral deposition, and increases as a result of collagen degradation, augmenting the exposure of carbonated hydroxylapatite (HAp) crystallites in the first stages of bone diagenesis. Because porosity is forty times higher in bone than in enamel (Wang and Cerling, 1994), the latter is widely accepted to be far more resistant to diagenesis than bone and is nowadays the tissue of reference for measuring trace elements concentration (Le Houedec et al., 2013; Joannes-Boyau et al., 2019; Nava et al., 2020; Funston et al., 2022) and/or isotope composition (Martin et al., 2014, 2015; Jaouen et al., 2017; McCormack et al., 2022).

In all types of tissue, some diagenetic overprints can be reverted using leaching pretreatment (Sillen and LeGeros, 1991; Koch et al., 1997; Nielsen-Marsh and Hedges, 2000; Balter et al., 2002a; Wathen et al., 2022). When formation of secondary mineral phases is thought to have occurred (additive-like diagenesis), leaching is potentially efficient at removing these minerals. One issue is that leaching is often performed in batch, leading samples to be leached more than necessary, therefore dissolving the most soluble HAp fraction that is the most pristine (Sillen and LeGeros, 1991; Balter et al., 2002a). The efficiency of the leaching method is even more questionable when diffusion of diagenetic elements (substitutive-like diagenesis) into the HAp has occurred.

All told, these considerations hold for trace elements, but the situation is unclear for major elements. Traditionally, the $\delta^{13}C$ and $\delta^{18}O$ values of CO_3 present in HAp (~5 wt%) are measured in leached samples due to the widespread presence of calcite in the porosity, but

the $\delta^{18}O$ value of HAp PO_4 (~55 wt%) is always measured in raw samples. The isotope composition of Ca of HAp (~40 wt%) varies according to trophic position (Skulan and DePaolo, 1999; Heuser et al., 2011; Martin et al., 2018; Hu et al., 2022) and physiology (Tacail et al., 2017; Hassler et al., 2021; Koutamanis et al., 2021; Li et al., 2022), but deserves an assessment of potential diagenetic effects on $\delta^{44/42}Ca$ values in bone and tooth enamel. Simple mass balance calculations already show that changes of the original $\delta^{44/42}Ca$ values in bone and tooth enamel by secondary Ca minerals are either small or would require an uncommonly fractionated Ca isotopes diagenetic pool (Heuser et al., 2011; Martin et al., 2017).

Here, we attempt to resolve this issue by studying how Ca isotopes behave during controlled experiments of artificial fossil bone and enamel leaching and in different diagenetic case studies. The Ca isotope compositions are measured along with Ca concentrations and Ca/P ratios to monitor the origin of Ca, and Rare Earth Elements (REE) to decipher the type (additive or substitutive) and extrapolate the extend of diagenetic alteration (Reynard et al., 1999; Trueman and Tuross, 2002).

2. Material and methods

First, we analyzed the Ca isotope composition in leached and unleached artificial samples mimicking fossil bone and enamel that have undergone an additive-like diagenesis. These samples consist of mixtures of HAp and calcite powder which $\delta^{44/42}Ca$ value are distinct and constrained. An artificial fossil bone was prepared using the bone ash certified reference material (SRM-1400, NIST; $\delta^{44/42}Ca$ = -1.21 ± 0.04‰, ± 2SD, n = 3) to which was added various proportions of the calcite certified reference material SRM-915b (NIST, $\delta^{44/42}Ca$ = -0.28 ± 0.04‰, ± 2SD, n = 21). The SRM-1400 certified reference material has been ashed and is devoid of organic matter and has a high crystallinity, both being characteristics of fossil bone. Because enamel certified reference material does not exist, we prepared artificial fossil enamel by mixing a sample of extant enamel from an isolated and partial molar tooth of modern elephant (*Elephas maximus;* $\delta^{44/42}Ca$ = -1.43 ± 0.07‰, ± 2SD, n = 10) with various proportions of SRM-915b. Second, we analyzed a suite of natural samples from different localities and ages that were selected according to their potential degree of diagenetic alteration. Pleistocene bone and tooth enamel samples were chosen to be representative of weak diagenesis, with preserved trace elements compositions, and Devonian bone of more

pronounced diagenesis. A first set of material is composed by a suite of fossil bone samples (n = 13) from the Camiac cave (Gironde, France). The site is a hyena dens from the upper Pleistocene (Mousterian period, 35.1 ± 2 ka BP; (Balter et al., 2002b). Taxonomic information is given in Table S2. This material is characterized by trace elements (Sr/Ca and Ba/Ca) distributions that reflect a trophic pattern (Balter et al., 2002b). A suite of fossil enamel samples (n = 14) from the Plio-Pleistocene of the Shungura Formation in the Lower Omo Valley (Ethiopia, sample age bracketed between 3.6 and 1.76 Ma; Boisserie et al., 2008) represents the second set of material. Here, the material is composed by only two extinct genera of large African suids (*Metridiochoerus* sp. and *Notochoerus* sp., Table S2). Leached fossil bone at Shungura exhibit Sr/Ca ratios characteristic of a trophic pattern (Sillen, 1986). A third set of samples gather vertebrate (fish and tetrapod) fossil bone (n = 25, Table S2) from the Devonian locality of Strud (360 Ma, Belgium; Olive et al., 2015). To our knowledge, no geochemical studies has already been performed on this material.

The samples were processed in the clean room and analyzed on the facilities at the Laboratoire de Géologie de Lyon: Terre, Planètes, Environnements (LGL-TPE, ENS de Lyon). All the samples (ca. ~ 5 mg) were leached using 0.5 ml of 0.1 M acetic acid per mg of sample during 30 min in an ultrasonic bath and rinsed with 18.2 MΩ/cm grade MilliQ water. This represents 2.5-fold the quantity of acid necessary to dissolve an equivalent amount of pure calcite. The samples were dissolved in distilled concentrated HNO_3 and an aliquot measured for major elements (P and Ca) by ICP-OES (Thermo Scientific, iCap 6000 Radial) and trace elements (REE) by ICP-MS (Thermo Scientific, iCap-Q) according to Balter and Lécuyer (2004). Calcium from the remaining solution was purified by ion-exchange chromatography and Ca isotope composition measured by MC-ICP-MS (Thermo Scientific, Neptune Plus) according to Tacail et al. (2014). Briefly, three ion-exchange chromatography steps are necessary, first allowing the recovery of Ca, Fe and Sr only, the second to purify Ca from Fe and the third to remove Sr (Table 1). Blanks for the procedure did not exceed 100 ng of Ca.

***Table 1**: Detailed procedure for Ca extraction and purification.*

1. Matrix elimination

AG50W-X12 resin (200-400 mesh) ~ 2 mL

Step	Eluent	Vol. (mL)
Condition	1 M HCl	10
Load	1 M HCl	2+1
Elution (matrix)	1 M HCl	55
Ca elution (Ca, Sr, Fe)	**6 M HCl**	**10**

2. Fe elimination if necessary

AG1-X8 resin (100-200 mesh) ~ 2 mL

Step	Eluent	Vol. (mL)
Condition	6 M HCl	10
Load	6 M HCl	1+1
Elution (Ca, Sr)	**6 M HCl**	**6**

3. Sr elimination

Sr-Specific resin (Eichrom) ~ 0.7 mL

Step	Eluent	Vol. (mL)
Condition	3 M HNO_3	5
Load	3 M HNO_3	0.5+0.5
Elution (Ca)	**3 M HNO_3**	**6**

Calcium isotope abundance ratios ($^{44}Ca/^{42}Ca$ and $^{43}Ca/^{42}Ca$) were measured using a Neptune Plus multi-collector ICP-MS using the standard-sample-standard bracketing method. All Ca isotope compositions are expressed using the delta notation, calculated as follows:

$$\delta^{44/42}\mathrm{Ca} = \left(\frac{(^{44}Ca/^{42}Ca_{\mathrm{Sample}})}{0.5 \times (^{44}Ca/^{42}Ca)^{n-1}_{ICP-Ca-Lyon} + 0.5 \times (^{44}Ca/^{42}Ca)^{n+1}_{ICP-Ca-Lyon}} - 1 \right) \times 1000$$

The ICP Ca Lyon standard, used routinely in Lyon, was used as the bracketing standard. The results can be converted relative to the SRM915a with an offset of -0.52‰.

3. Data presentation and interpretation

Results are given in Table S1 for artificial fossil bone and enamel and in Table S2 for natural fossil bone and enamel. The mass fractionation measured in this study agrees with the 0.5 slope predicted by the linear approximation of mass-dependent fractionation (Fig. S1).

We first test the effect of leaching on the $\delta^{44/42}$Ca value of the certified reference material SRM-1400 and found no difference after leaching ($\delta^{44/42}$Ca = -1.21 ± 0.03‰, ± 2SD, n = 3) compared to unleached material ($\delta^{44/42}$Ca = -1.21 ± 0.04‰, ± 2SD, n = 3). Absence of difference between the $\delta^{44/42}$Ca values of unleached and leached enamel is also observed as

154 we measured a constant $\delta^{44/42}$Ca value of -1.43‰ (Table S1). Because of the very small
155 amount of processed material (~ 5 mg), the remaining bone or enamel residue after leaching
156 is so small that it is impossible to weigh it, so Ca concentration for leached material is
157 underestimated. Nevertheless, using in 0.1 M acetic acid for 30 min generally leads to a loss
158 of about 30% of initial material. The absence of Ca isotope fractionation during leaching
159 therefore indicates that the dissolution of HAp is quantitative and that leaching *per se* does
160 not affect fossil bone and enamel $\delta^{44/42}$Ca values.

161 In the mixture of bone HAp with increasing proportion of added calcite, the slight
162 theoretical increase of Ca concentration is barely detected in unleached mixtures, probably
163 due to the ~5% error inherent to ICPMS measurements (Fig. 1A), but the decrease of Ca
164 content is inambiguous in leached mixture (Fig. 1A). In leached mixtures, the Ca content is
165 generally lower than predicted particularly for low calcite content (Fig. 1A). This suggests
166 partial dissolution of HAp that further occurs after complete dissolution of calcite (Balter et
167 al., 2002b). The leaching restores the Ca/P ratio of the mixture to the pure bone value (Fig.
168 1B). The leaching also restores the original bone $\delta^{44/42}$Ca value even up to 80% of added calcite
169 (Fig. 1C). The deviation of the bulk $\delta^{44/42}$Ca value can be detectable with ≥ 10% added calcite
170 and generally follows the theoretical balance between the HAp and the calcite end-members.
171

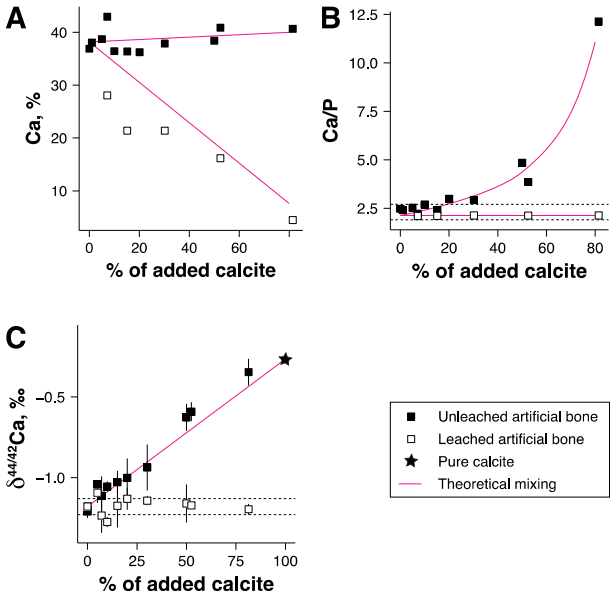

Fig. 1*: Effect of leaching on the Ca concentration (A), Ca/P ratio (B), and the* $\delta^{44/42}$*Ca (C) value of artificial fossil bone material (SRM-1400 + SRM-915b). Percentage of added calcite is relative to the initial total mass of the mixture. Error bars are typically < 5% in panel A. Dotted lines in panel B represent the natural range of the Ca/P ratio from 1.9 to 2.7 in biological HAp. Dotted lines in panel C represent the 2 standard deviations of the mean* $\delta^{44/42}$Ca *value of raw material. The* $\delta^{44/42}$*Ca value is reported relative to ICP-Ca Lyon.*

In the mixture of enamel with increasing proportion of calcite, the Ca concentration and Ca/P ratio between unleached and leached samples follow the same pattern than for bone (Fig. 2A, 2B). Dissolution of enamel is also observed for low calcite content as measured Ca concentrations stand below theoretical values (Fig. 2A). Similar to bone, deviation of the bulk $\delta^{44/42}$Ca value is detected with ≥ 10% added calcite, which follows the theoretical balance between the HAp and the calcite end-members, and leaching restores the initial enamel $\delta^{44/42}$Ca value even up to 80% of added calcite (Fig. 1C). Porosity in bone and enamel is variable (see Kral et al., 2021 for a discussion) but is grossly 40% in bone and one order of magnitude less (~1%) in enamel (Wang and Cerling, 1994). Given that bone and enamel can accommodate calcite to a magnitude equal to porosity, the results from artificial fossil bone and enamel suggest that the incorporation of calcite in natural fossil materials can be detected in the bone $\delta^{44/42}$Ca value but not for that enamel, except for unrealistic calcite $\delta^{44/42}$Ca value or important secondary porosity (e.g., post burial enamel surface cracks). This assumption is confirmed with results obtained on natural fossil bone and enamel.

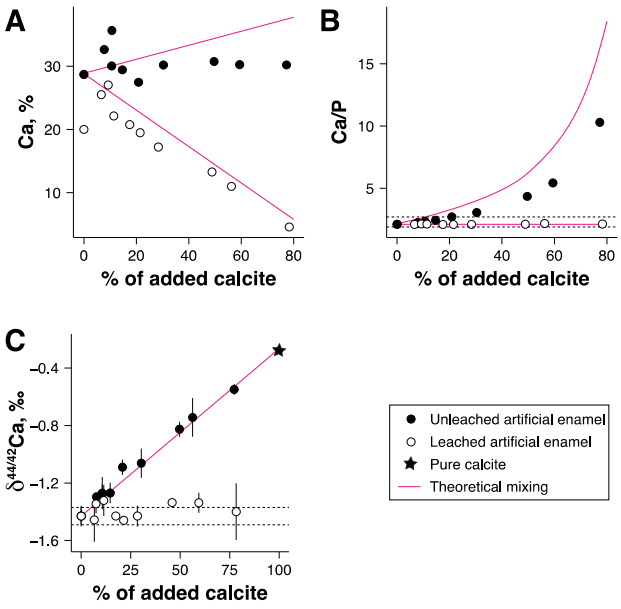

Fig. 2*: Effect of leaching on the Ca concentration (A), Ca/P ratio (B), and the* $\delta^{44/42}$*Ca (C) value of artificial fossil bone material (enamel + SRM-915b). Percentage of added calcite is relative to the initial total mass of the mixture. Error bars are typically < 5% in panel A. Dotted lines in panel B represent the natural range of the Ca/P ratio from 1.9 to 2.7 in biological HAp. Dotted lines in panel C represent the 2 standard deviations of the mean* $\delta^{44/42}$Ca *value of raw material. The* $\delta^{44/42}$*Ca value is reported relative to ICP-Ca Lyon.*

Fossil bone from Camiac (Table S2) shows a Ca/P decrease indicative of efficient removal of additive Ca of calcitic origin (Fig. 3A) along with a consistent decrease (-0.21 ± 0.11, n = 12) of the $\delta^{44/42}$Ca values during the leaching (Fig. 3B), validating the assumption that the added diagenetic Ca from calcite with a higher $\delta^{44/42}$Ca value than bone has been removed accordingly. Fossil enamel unleached and leached samples from Shungura (Table S2) show a Ca/P ratio that remains constant (Fig. 3C) and similar $\delta^{44/42}$Ca values (Fig. 3D), suggesting that non-significant amount of calcite was present in raw samples and that a quantitative fractionation of Ca isotopes occurred during leaching.

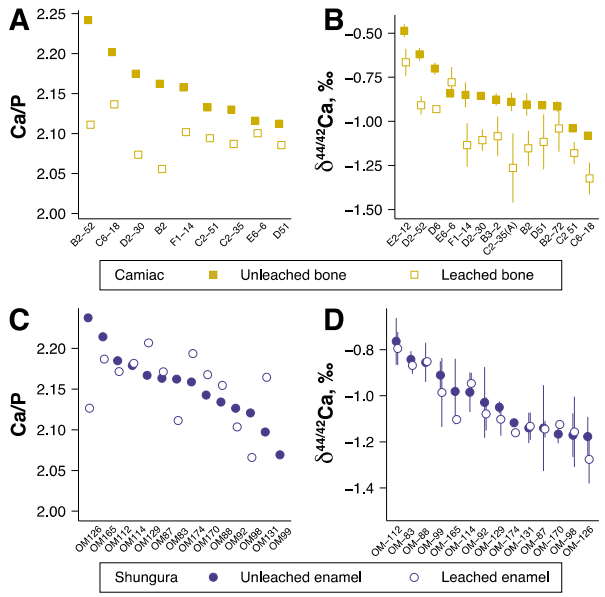

***Fig. 3**: Effect of leaching on the Ca/P ratio and $\delta^{44/42}$Ca value of natural fossil bone from Camiac (A and B) and fossil enamel from Shungura (C and D). The variability of the Ca/P ratio is in the natural range of the Ca/P ratio in biological Hap. The $\delta^{44/42}$Ca value is reported relative to ICP-Ca Lyon.*

Finally, the Devonian bone from Strud (Table S2) show invariable $\delta^{44/42}$Ca values with no preserved trophic information (Fig. 4) despite the leaching procedure. Here, the range of variation of the $\delta^{44/42}$Ca values (0.19‰, n = 25) is much more contracted than at Camiac (0.84‰, n = 26) or Shungura (0.51‰, n = 28). Note that Shungura samples are represented by two taxa of suids only (*Metridiochoerus* sp. and *Notochoerus* sp.), thus are not representative of the possible full trophic variability. The Ca/P range of variation at Strud (2.12 ± 0.07, ± 2SD, n = 25) is in the variability of biological HAp and does not indicate any Ca excess.

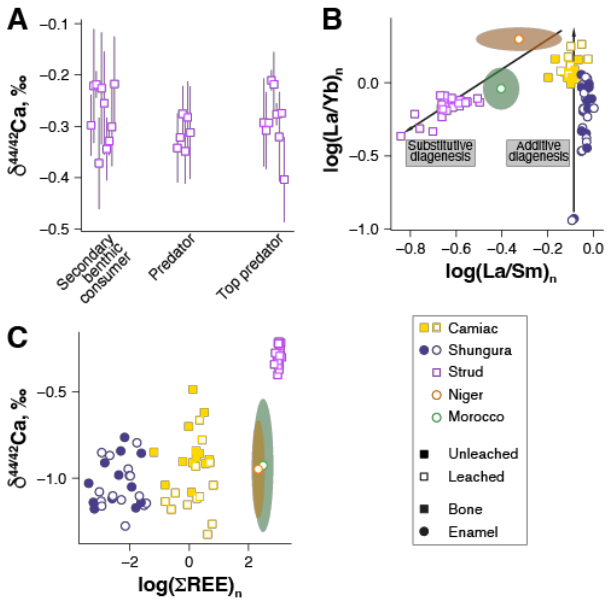

Fig. 4: (A) *$\delta^{44/42}$Ca values of leached bone at Strud. Trophic levels are assessed based on ecomorphological features. (B) $(La/Sm)_n$ vs $(La/Yb)_n$ distribution of fossil samples analyzed in the study. Morocco and Niger samples are from Hassler et al. (2018). REE have been normalized to PAAS. (C) $(\Sigma REE)_n$ vs $\delta^{44/42}$Ca distribution of fossil samples analyzed in the study. Morocco and Niger samples are from Hassler et al. (2018). REE have been normalized to PAAS. The $\delta^{44/42}$Ca value is reported relative to ICP-Ca Lyon.*

Taken together, the results of leaching experiments suggest that Ca isotopes in bone, but not in enamel, are sensitive to an additive-like diagenesis probably because bone porosity is high enough to accommodate significant amount of calcite to modify the original HAp $\delta^{44/42}$Ca value. In case of clear additive-like diagenesis (artificial fossil bone and enamel, Camiac fossil bone) the original HAp $\delta^{44/42}$Ca value is restored by leaching. However, in the case of the Strud fossil bones, the original HAp $\delta^{44/42}$Ca value cannot be restored by leaching as suggested by the absence of trophic pattern. At Strud, fossil bone probably experienced a substitutive-like diagenesis that was sufficiently pervasive to reset original HAp $\delta^{44/42}$Ca values.

4. Discussion

The type of fossil bone and enamel diagenesis, additive or substitutive, can be depicted by the REE pattern, and therefore help to detect whether the Ca isotope composition is potentially reset or not. REE trapping in fossil bone or enamel is a post-mortem phenomenon that occurs through two main processes, namely adsorption and substitution.

The suite of REE differs by ionic radius, middle REE (Sm) having an ionic radius close to that of Ca (~ 100 pm) and thus more liable to incorporate the HAp crystal lattice compared to light (La) or heavy (Yb) REE. The REE pattern can thus typify the nature of diagenetic processes because the relative partitioning among REE will be characteristic of the incorporation process. A quantitative incorporation without relative REE partitioning first occurs during early diagenesis, followed during protracted diagenesis by a non-quantitative adsorption mechanism controlled by surface crystal-chemical properties. Those mechanisms are considered additive in that the REE content increases during diagenesis, constituting an extra burden of trace elements that can be theoretically removed by leaching. While this assumption can be easily accepted concerning fossils that have undergone early diagenesis only, the efficiency of leaching is questionable in case of protracted diagenesis during which recrystallization inevitably occurred (Trueman and Tuross, 2002). Note that Hap recrystallisation, as witnessed by the increase of crystallite size can occur within a few years post-mortem (Trueman et al., 2004), but is linked to the exposure of HAp crystallite surfaces during the breakdown of collagen (Trueman et al., 2008). Finally, a substitution mechanism, which is controlled by bulk crystal-chemical properties, can occur during extensive diagenesis, leading to strong REE partitioning (Reynard et al., 1999), along with progressive transformation of HAp into francolite (Trueman and Tuross, 2002). The effects of this late-stage substitutive-like diagenesis are anticipated to be insensitive to leaching.

As expected, the Late Pleistocene Camiac bone and Early Pleistocene Shungura enamel samples exhibit $(La/Sm)_n$ and $(La/Yb)_n$ ratios characteristic of early diagenesis, supporting the idea that well preserved $\delta^{44/42}Ca$ values (Fig. 4B) can be obtained in leached samples, which is necessary for bone (Fig. 3B) but not for enamel (Fig. 3D) due to the presence of secondary Ca-carbonate in bone but not in enamel. Leaching has no influence on the $(La/Sm)_n$ and $(La/Yb)_n$ ratios for both bone from Camiac and enamel from Shungura (Table S2). The REE pattern at Strud is indicative of a substitutive-like diagenesis (Fig. 4B), and despite leaching, the associated bone $\delta^{44/42}Ca$, which are contracted and invariable among trophic positions, are reset by diagenesis. The picture is however different for fossil enamel. For instance, Cretaceous dinosaur enamel samples from Hassler et al. (2018), which have not been leached, still exhibit highly variable $\delta^{44/42}Ca$ values (from -1.6‰ to -0.4‰) with preserved trophic systematics, despite obvious signs of substitutive-like diagenesis, i.e., hat-shaped REE patterns (Hassler et al., 2018) and low $(La/Sm)_n$ ratios (Fig. 4B). Fossil bone or

277 enamel are open systems and accumulate REE during diagenesis, being through the
278 adsorption and/or the substitution processes. The REE concentration $(\Sigma REE)_n$ thus increases
279 during diagenesis, spanning four orders of magnitude between Shungura enamel samples
280 (0.009 ± 0.020 μg/g, ± 2SD, n = 28, Table S2) and Strud bone samples (1028 ± 724 μg/g, ± 2SD,
281 n = 25, Table S2, Fig. 4C). Dinosaurs enamel samples from Morocco (417 ± 581 μg/g, ± 2SD, n
282 = 23) and from Niger (237 ± 282 μg/g, ± 2SD, n = 49) display high $(\Sigma REE)_n$ concentrations, but
283 still variable $\delta^{44/42}$Ca values despite the absence of leaching.

284 The substitutive-like REE pattern is thus not a good proxy of Ca isotope extended
285 diagenesis in fossil enamel. An explanation is that the enamel one percent of porosity is
286 insufficient to accommodate enough Ca in diagenetic fluids and/or secondary minerals that
287 will further substitute with HAp to significantly modify the isotopic composition of the enamel
288 bulk Ca. This assumption holds providing a realistic $\delta^{44/42}$Ca value of the diagenetic pool (fluid
289 or mineral), which must stand close to the value of river water, i.e., ~0‰ (Heuser et al., 2011;
290 Martin et al., 2017). A simple mass balance calculation indicates that a 1% porosity full of Ca
291 necessitates the diagenetic pool to be ± 4‰ different from the HAp to modify the $\delta^{44/42}$Ca
292 value by ± 0.1‰. In bone, the situation is clearly different because the porosity (~40%) grossly
293 equals the HAp Ca content, so the diagenetic pool can have realistic $\delta^{44/42}$Ca value, i.e., close
294 to that of HAp. Taking all the above results into account, we conclude that Ca isotopes are
295 largely immune to diagenesis in fossil enamel, but not in fossil bone.
296
297 **5. Conclusion**

298 We demonstrate that an addition of a diagenetic phase containing Ca in the form of
299 Ca-carbonate significantly modifies the bulk $\delta^{44/42}$Ca value of artificial fossil bone and enamel,
300 whose initial composition can be restored using leaching. For fossils that have undergone
301 weak diagenesis, this process is reproduced in fossil bone, but not in fossil enamel, which
302 cannot accommodate enough diagenetic Ca in the porosity to modify the bulk $\delta^{44/42}$Ca value.
303 For fossils that have undergone extensive diagenesis, as typified by the REE patterns, leaching
304 is unable to restore the initial bone $\delta^{44/42}$Ca value, while enamel can still contain non-
305 significantly modified $\delta^{44/42}$Ca values, even in the absence of leaching. The diagenetic Ca
306 content that can be added in the porosity during early diagenesis of enamel is too low and is
307 further unable to modify its bulk $\delta^{44/42}$Ca value by substitution. The REE pattern of fossil

enamel is thus not a reliable proxy for extensive diagenetic alteration of Ca isotopes, which remains to be potentially uncovered by crystal-chemical means.

Declaration of competing interest

The authors declare that they have no known competing financial interests or personal relationships that could have appeared to influence the work reported in this paper.

Acknowledgements

Pierre-Jean Dodat received financial supports from the CNRS 80|PRIME program and Research Program of the Nouvelle Aquitaine Region: Isotopes du calcium et anthropobiologie au Paléolithique moyen, convention n° 2019-1R40208. Sébastien Olive received funding from Fonds de la recherche scientifique (FNRS) and the European Union's Horizon 2020 research and innovation programme under the Marie Sklodowska-Curie grant agreement No 101032456-TNT. Kani Bayez, Gaël Clément, Cécilia Cousin, Valentin Fischer, Annelise Folie, Emmanuel Robert, and the Omo Group Research Expedition (OGRE) are thanked for helping with the processing of fossil samples. Sampling authorization was delivered to the OGRE by the Ethiopian Heritage Authority/National Museum of Ethiopia, and a fossil sampling session in Addis Ababa was funded by the project ANR-17-CE27-0002 'DietScratches'. We thank two anonymous reviewers and the Associate Editor Adrian Immenhauser for their in-depth reviews and constructive comments that greatly improve the quality of this article.

Appendix A. Supplementary material

Supplementary figure 1: Mass fractionation in three-isotope space $\delta^{43/42}$Ca vs $\delta^{44/42}$Ca calculated from the measurements of the samples in this study.

Supplementary table 1: Table of results for artificial fossil bone and enamel samples.

Supplementary table 2: Table of results for natural fossil bone and enamel samples.

References

Balter, V., Bocherens, H., Person, A., Labourdette, N., Renard, M., Vandermeersch, B., 2002a. Ecological and physiological variability of Sr/Ca and Ba/Ca in mammals of

West European mid-Würmian food webs. Palaeogeogr., Palaeoclimatol., Palaeoecol. 186, 127–143.

Balter, V., Saliège, J.–F., Bocherens, H., Person, A., 2002b. Evidence of physico–chemical and isotopic modifications in archaeological bones during controlled acid etching. Archaeometry 44, 329–336.

Balter, V., Lécuyer, C., 2004. Determination of Sr and Ba partition coefficients between apatite and water from 5°C to 60°C: a potential new thermometer for aquatic paleoenvironments. Geochim. Cosmochim. Acta 68, 423–432.

Boisserie, J.-R., Guy, F., Delagnes, A., Hlukso, L.J., Bibi, F., Beyene, Y., Guillemot, C., 2008. New palaeoanthropological research in the Plio-Pleistocene Omo Group, Lower Omo Valley, SNNPR (Southern Nations, Nationalities and People Regions), Ethiopia. C. R. Palevol 7, 429–439.

Funston, G.F., dePolo, P.E., Sliwinski, J.T., Dumont, M., Shelley, S.L., Pichevin, L.E., Cayzer, N.J., Wible, J.R., Williamson, T.E., Rae, J.W.B., Brusatte, S.L., 2022. The origin of placental mammal life histories. Nature 610, 107–111.

Hassler, A., Martin, J.E., Amiot, R., Tacail, T., Godet, F.A., Allain, R., Balter, V., 2018. Calcium isotopes offer clues on resource partitioning among Cretaceous predatory dinosaurs. Proc. R. Soc. B 285, 20180197.

Hassler, A., Martin, J.E., Merceron, G., Garel, M., Balter, V., 2021. Calcium isotopic variability of cervid bioapatite and implications for mammalian physiology and diet. Palaeogeogr., Palaeoclimatol., Palaeoecol. 573, 110418.

Hedges, R.E.M., 2002. Bone diagenesis: an overview of processes. Archaeometry 44, 319–328.

Heuser, A., Tütken, T., Gussone, N., Galer, S.J.G., 2011. Calcium isotopes in fossil bones and teeth — Diagenetic versus biogenic origin. Geochim. Cosmochim. Acta 75, 3419–3433.

Hu, Y., Jiang, Q., Liu, F., Guo, L., Zhang, Z., Zhao, L., 2022. Calcium isotope ecology of early Gigantopithecus blacki (∼2 Ma) in South China. Earth Planet. Sci. Lett. 584, 117522.

Jaouen, K., Herrscher, E., Balter, V., 2017. Copper and zinc isotope ratios in human bone and enamel. Am. J. Phys. Anthropol. 162, 491–500.

Joannes-Boyau, R., Adams, J.W., Austin, C., Arora, M., Moffat, I., Herries, A.I.R., Tonge, M.P., Benazzi, S., Evans, A.R., Kullmer, O., Wroe, S., Dosseto, A., Fiorenza, L., 2019. Elemental signatures of Australopithecus africanus teeth reveal seasonal dietary stress. Nature 572, 112–115.

Koch, P.L., Tuross, N., Fogel, M.L., 1997. The Effects of Sample Treatment and Diagenesis on the Isotopic Integrity of Carbonate in Biogenic Hydroxylapatite. J. Archaeol. Sci. 24, 417–429.

376 Kohn, M.J., Moses, R.J., 2013. Trace element diffusivities in bone rule out simple diffusive
377 uptake during fossilization but explain in vivo uptake and release. Proc. Natl. Acad.
378 Sci. USA 110, 419–424.

379 Koutamanis, D., Roberts, G.L., Dosseto, A., 2021. Inter- and intra-individual variability of
380 calcium and strontium isotopes in modern Tasmanian wombats. Palaeogeogr.,
381 Palaeoclimatol., Palaeoecol. 574, 110435.

382 Kral, A.G., Lagos, M., Guagliardo, P., Tütken, T., Geisler, T., 2022. Rapid alteration of cortical
383 bone in fresh- and seawater solutions visualized and quantified from the millimeter
384 down to the atomic scale. Chem. Geol. 609, 121060.

385 Kral, A.G., Ziegler, A., Tütken, T., Geisler, T., 2021. Experimental aqueous alteration of
386 cortical bone microarchitecture analyzed by quantitative micro-computed
387 tomography. Front Earth Sci 9, 609496.

388 Le Houedec, S., Girard, C., Balter, V., 2013. Conodont Sr/Ca and $\delta^{18}O$ record seawater
389 changes at the Frasnian–Famennian boundary. Palaeogeogr., Palaeoclimatol.,
390 Palaeoecol. 376, 114–121.

391 Li, Q., Nava, A., Reynard, L.M., Thirlwall, M., Bondioli, L., Müller, W., 2022. Spatially-
392 Resolved Ca Isotopic and Trace Element Variations in Human Deciduous Teeth
393 Record Diet and Physiological Change. Environ. Archaeol. 27, 474–483.

394 Martin, J.E., Deesri, U., Liard, R., Wattanapituksakul, A., Suteethorn, S., Lauprasert, K., Tong,
395 H., Buffetaut, E., Suteethorn, V., Suan, G., Télouk, P., Balter, V., 2015. Strontium
396 isotopes and the long-term residency of thalattosuchians in the freshwater
397 environment. Paleobiology 42, 143–156.

398 Martin, J.E., Tacail, T., Balter, V., 2017. Non-traditional isotope perspectives in vertebrate
399 palaeobiology. Palaeontology 60, 485–502.

400 Martin, J.E., Tacail, T., Cerling, T.E., Balter, V., 2018. Calcium isotopes in enamel of modern
401 and Plio-Pleistocene East African mammals. Earth Planet. Sci. Lett. 503, 227–235.

402 Martin J.E., Vance, D., Balter, V., 2014. Natural variation of magnesium isotopes in mammal
403 bones and teeth from two South African trophic chains. Geochim. Cosmochim. Acta
404 130, 12–20.

405 McCormack, J., Griffiths, M.L., Kim, S.L., Shimada, K., Karnes, M., Maisch, H., Pederzani, S.,
406 Bourgon, N., Jaouen, K., Becker, M.A., Jöns, N., Sisma-Ventura, G., Straube, N.,
407 Pollerspöck, J., Hublin, J.-J., Eagle, R.A., Tütken, T., 2022. Trophic position of Otodus
408 megalodon and great white sharks through time revealed by zinc isotopes. Nat.
409 Comm. 13, 2980.

410 Nava, A., Lugli, F., Romandini, M., Badino, F., Evans, D., Helbling, A. H., Oxilia, G., Arrighi, S.,
411 Bortolini, E., Delpiano, D., Duches, R., Figus, C., Livraghi, A., Marciani, G., Silvestrini,
412 S., Cipriani, A., Giovanardi, T., Pini, R., Tuniz, C., Bernardini, F., Dori, I., Coppa, A.,

413 Cristiani, E., Dean, C., Bondioli, L., Peresani, M., Müller, W., Benazzi, S., 2020. Early
414 life of Neanderthals. Proc. Natl. Acad. Sci. USA 117, 28719–28726.

415 Nielsen-Marsh, C.M., Hedges, R.E.M., 2000. Patterns of Diagenesis in Bone I: The Effects of
416 Site Environments. J. Archaeol. Sci. 27, 1139–1150.

417 Olive, S., Clément, G., Daeschler, E.B., Dupret, V., 2015. Characterization of the placoderm
418 (Gnathostomata) assemblage from the tetrapod-bearing locality of Strud (Belgium,
419 upper Famennian). Palaeontology 58, 981–1002.

420 Reynard, B., Lécuyer, C., Grandjean, P., 1999. Crystal-chemical controls on rare-earth
421 element concentrations in fossil biogenic apatites and implications for
422 paleoenvironmental reconstructions. Chem. Geol. 155, 233–241.

423 Sillen, A., 1986. Biogenic and Diagenetic Sr/Ca in Plio-Pleistocene Fossils of the Omo
424 Shungura Formation. Paleobiology 12, 311–323.

425 Sillen, A., LeGeros, R., 1991. Solubility profiles of synthetic apatites and of modern and fossil
426 bones. J. Archaeol. Sci. 18, 385–397.

427 Skulan, J., DePaolo D.J., 1999. Calcium isotope fractionation between soft and mineralized
428 tissues as a monitor of calcium use in vertebrates. Proc. Natl. Acad. Sci. USA 96,
429 13709–13713.

430 Suarez, C.A., Kohn, M.J., 2020. Caught in the act: A case study on microscopic scale
431 physicochemical effects of fossilization on stable isotopic composition of bone.
432 Geochim. Cosmochim. Acta 268, 277–295.

433 Tacail, T., Albalat, E., Télouk, P., Balter, V., 2014. A simplified protocol for measurement of
434 Ca isotopes in biological samples. J. Anal. At. Spectrom. 29, 529.

435 Tacail, T., Thivichon-Prince, B., Martin, J.E., Charles, C., Viriot, L., Balter, V., 2017. Assessing
436 human weaning practices with calcium isotopes in tooth enamel. Proc. Natl. Acad.
437 Sci. USA 114, 6268–6273.

438 Trueman, C.N.G., Behrensmeyer, A.K., Tuross, N., Weiner, S., 2004. Mineralogical and
439 compositional changes in bones exposed on soil surfaces in Amboseli National Park,
440 Kenya: diagenetic mechanisms and the role of sediment pore fluids. J. Archaeol. Sci.
441 31, 721–739.

442 Trueman, C.N., Privat, K., Field, J., 2008. Why do crystallinity values fail to predict the extent
443 of diagenetic alteration of bone mineral? Palaeogeogr., Palaeoclimatol., Palaeoecol.
444 266, 160–167.

445 Trueman, C.N., Tuross, N., 2002. Trace Elements in Recent and Fossil Bone Apatite. Rev.
446 Mineral. Geochem. 48, 489–521.

447 Wang, Y., Cerling, T.E., 1994. A model of fossil tooth and bone diagenesis: implications for
448 paleodiet reconstruction from stable isotopes. Palaeogeogr., Palaeoclimatol.,
449 Palaeoecol. 107, 281–289.

450 Wathen, C. A., Isaksson, S., Lidén, K., 2022. On the road again—a review of pretreatment
451 methods for the decontamination of skeletal materials for strontium isotopic and
452 concentration analysis. Archaeol. Anthropol. Sci. 14, 45.

453 Weber, K., Weber, M., Menneken, M., Kral, A. G., Mertz-Kraus, R., Geisler, T., Vogl, J.,
454 Tütken, T., 2021. Diagenetic stability of non-traditional stable isotope systems (Ca,
455 Sr, Mg, Zn) in teeth – An in-vitro alteration experiment of biogenic apatite in
456 isotopically enriched tracer solution. Chem. Geol. 572, 120196.

457

Limits of calcium isotopes diagenesis in fossil bone and enamel

Pierre-Jean Dodat [1,2], Jeremy E. Martin [1], Sébastien Olive [1,3], Auguste Hassler[1,4,5], Emmanuelle Albalat [1], Jean-Renaud Boisserie [6,7], Gildas Merceron [6], Antoine Souron [2], Bruno Maureille [2], Vincent Balter [1,*]

1 : LGL-TPE, UMR 5276, ENS de Lyon, CNRS, Univ. Lyon 1. 46 Allée d'Italie, 69342 Lyon Cedex 07, France.0

2 : PACEA UMR 5199, Univ. Bordeaux, CNRS, MC, F-33600 Pessac France.

3 : Directorate Earth & Life History, Royal Belgian Institute of Natural Sciences, Rue Vautier 29, 1000 Brussels, Belgium

4 : Present address: Department of Archaeology, University of Aberdeen, Aberdeen, United Kingdom

5 : Present address: Department of Earth and Environmental Sciences, University of Ottawa, Ottawa, ON, Canada.

6 : PALEVOPRIM, UMR 7262, CNRS, Univ. Poitiers, 86073 Poitiers, France

7 : CFEE UAR 3137, CNRS, Ministère de l'Europe et des affaires étrangères, PO BOX 5554 Addis Ababa, Ethiopia

* Corresponding author: vincent.balter@ens-lyon.fr

Abstract

Diagenesis has been recognized for decades to significantly alter the trace elements biogenic signatures in fossil tooth enamel and bone that are routinely used for paleobiological and paleoenvironmental reconstructions. This signature is modified during diagenesis according to a complex continuum between two main processes, addition, and substitution. For an additive-like, or early diagenesis, the trace elements biogenic profiles can be restored by leaching secondary minerals, but this technique is inefficient for a substitutive-like, or extensive diagenesis for which secondary trace elements are incorporated into the biogenic mineral. This scheme is however unclear for Ca, the major cation in tooth enamel and bone hydroxylapatite, which stable isotope composition ($\delta^{44/42}$Ca) also conveys biological and environmental information. We present a suite of leaching experiments for monitoring $\delta^{44/42}$Ca values in artificial and natural fossil enamel and bone from different settings. The results show that enamel $\delta^{44/42}$Ca values are insensitive to an additive-like diagenesis that involves the formation of secondary Ca-carbonate mineral phases, while bone shows a consistent offset toward ^{44}Ca-enriched values, that can be restored to the biogenic baseline by a leaching procedure. In the context of a substitutive-like diagenesis, bone exhibits constant $\delta^{44/42}$Ca values, insensitive to leaching, and shows a REE pattern symptomatic of extensive diagenesis. Such a REE pattern can be observed in fossil enamel for which $\delta^{44/42}$Ca values are still fluctuating and follow a trophic pattern. We conclude that Ca isotopes in fossil enamel are probably not prone to extensive diagenesis and argue that this immunity is due to the very low porosity of enamel that cannot accommodate enough secondary minerals to significantly modify the isotopic composition of the enamel Ca pool.

1. Introduction

Bone, dentin, and enamel are valuable archives for recording information about the life history and environment of fossil and extant vertebrates. The information is embedded as trace elements or isotopic ratios signature during the genesis of the mineralized tissue, a signature that is further obfuscated by diagenesis during fossilization. Regarding trace elements, the comprehension of diagenetic mechanisms has greatly benefited from in-situ laser ablation measurements (Kohn and Moses, 2013; Kral et al., 2022), highlighting the complex interplay of the diffusion, adsorption, and transport reaction processes. However, while sophisticated techniques are now deployed to fully integrate all the hallmarks of diagenesis (Suarez and Kohn, 2020; Weber et al., 2021; Kral et al., 2022), the results still recognize the central importance of porosity which was already suspected in the 2000's (Hedges, 2002; Trueman and Tuross, 2002; Kral et al., 2021). Porosity mediates fluid circulation and secondary mineral deposition, and increases as a result of collagen degradation, augmenting the exposure of carbonated hydroxylapatite (HAp) crystallites in the first stages of bone diagenesis. Because porosity is forty times higher in bone than in enamel (Wang and Cerling, 1994), the latter is widely accepted to be far more resistant to diagenesis than bone and is nowadays the tissue of reference for measuring trace elements concentration (Le Houedec et al., 2013; Joannes-Boyau et al., 2019; Nava et al., 2020; Funston et al., 2022) and/or isotope composition (Martin et al., 2014, 2015; Jaouen et al., 2017; McCormack et al., 2022).

In all types of tissue, some diagenetic overprints can be reverted using leaching pretreatment (Sillen and LeGeros, 1991; Koch et al., 1997; Nielsen-Marsh and Hedges, 2000; Balter et al., 2002a; Wathen et al., 2022). When formation of secondary mineral phases is thought to have occurred (additive-like diagenesis), leaching is potentially efficient at removing these minerals. One issue is that leaching is often performed in batch, leading samples to be leached more than necessary, therefore dissolving the most soluble HAp fraction that is the most pristine (Sillen and LeGeros, 1991; Balter et al., 2002a). The efficiency of the leaching method is even more questionable when diffusion of diagenetic elements (substitutive-like diagenesis) into the HAp has occurred.

All told, these considerations hold for trace elements, but the situation is unclear for major elements. Traditionally, the $\delta^{13}C$ and $\delta^{18}O$ values of CO_3 present in HAp (~5 wt%) are measured in leached samples due to the widespread presence of calcite in the porosity, but

the $\delta^{18}O$ value of HAp PO_4 (~55 wt%) is always measured in raw samples. The isotope composition of Ca of HAp (~40 wt%) varies according to trophic position (Skulan and DePaolo, 1999; Heuser et al., 2011; Martin et al., 2018; Hu et al., 2022) and physiology (Tacail et al., 2017; Hassler et al., 2021; Koutamanis et al., 2021; Li et al., 2022), but deserves an assessment of potential diagenetic effects on $\delta^{44/42}Ca$ values in bone and tooth enamel. Simple mass balance calculations already show that changes of the original $\delta^{44/42}Ca$ values in bone and tooth enamel by secondary Ca minerals are either small or would require an uncommonly fractionated Ca isotopes diagenetic pool (Heuser et al., 2011; Martin et al., 2017).

Here, we attempt to resolve this issue by studying how Ca isotopes behave during controlled experiments of artificial fossil bone and enamel leaching and in different diagenetic case studies. The Ca isotope compositions are measured along with Ca concentrations and Ca/P ratios to monitor the origin of Ca, and Rare Earth Elements (REE) to decipher the type (additive or substitutive) and extrapolate the extend of diagenetic alteration (Reynard et al., 1999; Trueman and Tuross, 2002).

2. Material and methods

First, we analyzed the Ca isotope composition in leached and unleached artificial samples mimicking fossil bone and enamel that have undergone an additive-like diagenesis. These samples consist of mixtures of HAp and calcite powder which $\delta^{44/42}Ca$ value are distinct and constrained. An artificial fossil bone was prepared using the bone ash certified reference material (SRM-1400, NIST; $\delta^{44/42}Ca$ = -1.21 ± 0.04‰, ± 2SD, n = 3) to which was added various proportions of the calcite certified reference material SRM-915b (NIST, $\delta^{44/42}Ca$ = -0.28 ± 0.04‰, ± 2SD, n = 21). The SRM-1400 certified reference material has been ashed and is devoid of organic matter and has a high crystallinity, both being characteristics of fossil bone. Because enamel certified reference material does not exist, we prepared artificial fossil enamel by mixing a sample of extant enamel from an isolated and partial molar tooth of modern elephant (*Elephas maximus;* $\delta^{44/42}Ca$ = -1.43 ± 0.07‰, ± 2SD, n = 10) with various proportions of SRM-915b. Second, we analyzed a suite of natural samples from different localities and ages that were selected according to their potential degree of diagenetic alteration. Pleistocene bone and tooth enamel samples were chosen to be representative of weak diagenesis, with preserved trace elements compositions, and Devonian bone of more

pronounced diagenesis. A first set of material is composed by a suite of fossil bone samples (n = 13) from the Camiac cave (Gironde, France). The site is a hyena dens from the upper Pleistocene (Mousterian period, 35.1 ± 2 ka BP; (Balter et al., 2002b). Taxonomic information is given in Table S2. This material is characterized by trace elements (Sr/Ca and Ba/Ca) distributions that reflect a trophic pattern (Balter et al., 2002b). A suite of fossil enamel samples (n = 14) from the Plio-Pleistocene of the Shungura Formation in the Lower Omo Valley (Ethiopia, sample age bracketed between 3.6 and 1.76 Ma; Boisserie et al., 2008) represents the second set of material. Here, the material is composed by only two extinct genera of large African suids (*Metridiochoerus* sp. and *Notochoerus* sp., Table S2). Leached fossil bone at Shungura exhibit Sr/Ca ratios characteristic of a trophic pattern (Sillen, 1986). A third set of samples gather vertebrate (fish and tetrapod) fossil bone (n = 25, Table S2) from the Devonian locality of Strud (360 Ma, Belgium; Olive et al., 2015). To our knowledge, no geochemical studies has already been performed on this material.

The samples were processed in the clean room and analyzed on the facilities at the Laboratoire de Géologie de Lyon: Terre, Planètes, Environnements (LGL-TPE, ENS de Lyon). All the samples (ca. ~ 5 mg) were leached using 0.5 ml of 0.1 M acetic acid per mg of sample during 30 min in an ultrasonic bath and rinsed with 18.2 MΩ/cm grade MilliQ water. This represents 2.5-fold the quantity of acid necessary to dissolve an equivalent amount of pure calcite. The samples were dissolved in distilled concentrated HNO_3 and an aliquot measured for major elements (P and Ca) by ICP-OES (Thermo Scientific, iCap 6000 Radial) and trace elements (REE) by ICP-MS (Thermo Scientific, iCap-Q) according to Balter and Lécuyer (2004). Calcium from the remaining solution was purified by ion-exchange chromatography and Ca isotope composition measured by MC-ICP-MS (Thermo Scientific, Neptune Plus) according to Tacail et al. (2014). Briefly, three ion-exchange chromatography steps are necessary, first allowing the recovery of Ca, Fe and Sr only, the second to purify Ca from Fe and the third to remove Sr (Table 1). Blanks for the procedure did not exceed 100 ng of Ca.

***Table 1**: Detailed procedure for Ca extraction and purification.*

1. Matrix elimination

AG50W-X12 resin (200-400 mesh) ~ 2 mL

Step	Eluent	Vol. (mL)
Condition	1 M HCl	10
Load	1 M HCl	2+1
Elution (matrix)	1 M HCl	55
Ca elution (Ca, Sr, Fe)	**6 M HCl**	**10**

2. Fe elimination if necessary

AG1-X8 resin (100-200 mesh) ~ 2 mL

Step	Eluent	Vol. (mL)
Condition	6 M HCl	10
Load	6 M HCl	1+1
Elution (Ca, Sr)	**6 M HCl**	**6**

3. Sr elimination

Sr-Specific resin (Eichrom) ~ 0.7 mL

Step	Eluent	Vol. (mL)
Condition	3 M HNO_3	5
Load	3 M HNO_3	0.5+0.5
Elution (Ca)	**3 M HNO_3**	**6**

Calcium isotope abundance ratios ($^{44}Ca/^{42}Ca$ and $^{43}Ca/^{42}Ca$) were measured using a Neptune Plus multi-collector ICP-MS using the standard-sample-standard bracketing method. All Ca isotope compositions are expressed using the delta notation, calculated as follows:

$$\delta^{44/42}\mathrm{Ca} = \left(\frac{(^{44}Ca/^{42}Ca_{\mathrm{Sample}})}{0.5 \times (^{44}Ca/^{42}Ca)^{n-1}_{ICP-Ca-Lyon} + 0.5 \times (^{44}Ca/^{42}Ca)^{n+1}_{ICP-Ca-Lyon}} - 1 \right) \times 1000$$

The ICP Ca Lyon standard, used routinely in Lyon, was used as the bracketing standard. The results can be converted relative to the SRM915a with an offset of -0.52‰.

3. Data presentation and interpretation

Results are given in Table S1 for artificial fossil bone and enamel and in Table S2 for natural fossil bone and enamel. The mass fractionation measured in this study agrees with the 0.5 slope predicted by the linear approximation of mass-dependent fractionation (Fig. S1).

We first test the effect of leaching on the $\delta^{44/42}$Ca value of the certified reference material SRM-1400 and found no difference after leaching ($\delta^{44/42}$Ca = -1.21 ± 0.03‰, ± 2SD, n = 3) compared to unleached material ($\delta^{44/42}$Ca = -1.21 ± 0.04‰, ± 2SD, n = 3). Absence of difference between the $\delta^{44/42}$Ca values of unleached and leached enamel is also observed as

154 we measured a constant $\delta^{44/42}$Ca value of -1.43‰ (Table S1). Because of the very small
155 amount of processed material (~ 5 mg), the remaining bone or enamel residue after leaching
156 is so small that it is impossible to weigh it, so Ca concentration for leached material is
157 underestimated. Nevertheless, using in 0.1 M acetic acid for 30 min generally leads to a loss
158 of about 30% of initial material. The absence of Ca isotope fractionation during leaching
159 therefore indicates that the dissolution of HAp is quantitative and that leaching *per se* does
160 not affect fossil bone and enamel $\delta^{44/42}$Ca values.
161 In the mixture of bone HAp with increasing proportion of added calcite, the slight
162 theoretical increase of Ca concentration is barely detected in unleached mixtures, probably
163 due to the ~5% error inherent to ICPMS measurements (Fig. 1A), but the decrease of Ca
164 content is inambiguous in leached mixture (Fig. 1A). In leached mixtures, the Ca content is
165 generally lower than predicted particularly for low calcite content (Fig. 1A). This suggests
166 partial dissolution of HAp that further occurs after complete dissolution of calcite (Balter et
167 al., 2002b). The leaching restores the Ca/P ratio of the mixture to the pure bone value (Fig.
168 1B). The leaching also restores the original bone $\delta^{44/42}$Ca value even up to 80% of added calcite
169 (Fig. 1C). The deviation of the bulk $\delta^{44/42}$Ca value can be detectable with ≥ 10% added calcite
170 and generally follows the theoretical balance between the HAp and the calcite end-members.
171

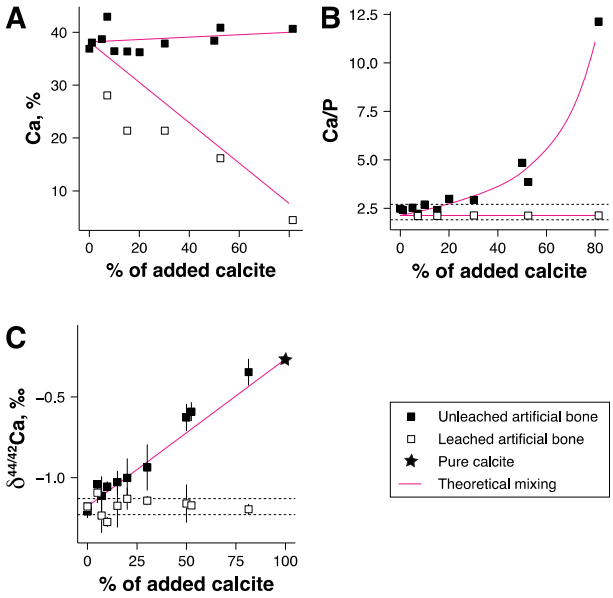

Fig. 1*: Effect of leaching on the Ca concentration (A), Ca/P ratio (B), and the* $\delta^{44/42}$*Ca (C) value of artificial fossil bone material (SRM-1400 + SRM-915b). Percentage of added calcite is relative to the initial total mass of the mixture. Error bars are typically < 5% in panel A. Dotted lines in panel B represent the natural range of the Ca/P ratio from 1.9 to 2.7 in biological HAp. Dotted lines in panel C represent the 2 standard deviations of the mean* $\delta^{44/42}$Ca *value of raw material. The* $\delta^{44/42}$*Ca value is reported relative to ICP-Ca Lyon.*

In the mixture of enamel with increasing proportion of calcite, the Ca concentration and Ca/P ratio between unleached and leached samples follow the same pattern than for bone (Fig. 2A, 2B). Dissolution of enamel is also observed for low calcite content as measured Ca concentrations stand below theoretical values (Fig. 2A). Similar to bone, deviation of the bulk $\delta^{44/42}$Ca value is detected with ≥ 10% added calcite, which follows the theoretical balance between the HAp and the calcite end-members, and leaching restores the initial enamel $\delta^{44/42}$Ca value even up to 80% of added calcite (Fig. 1C). Porosity in bone and enamel is variable (see Kral et al., 2021 for a discussion) but is grossly 40% in bone and one order of magnitude less (~1%) in enamel (Wang and Cerling, 1994). Given that bone and enamel can accommodate calcite to a magnitude equal to porosity, the results from artificial fossil bone and enamel suggest that the incorporation of calcite in natural fossil materials can be detected in the bone $\delta^{44/42}$Ca value but not for that enamel, except for unrealistic calcite $\delta^{44/42}$Ca value or important secondary porosity (e.g., post burial enamel surface cracks). This assumption is confirmed with results obtained on natural fossil bone and enamel.

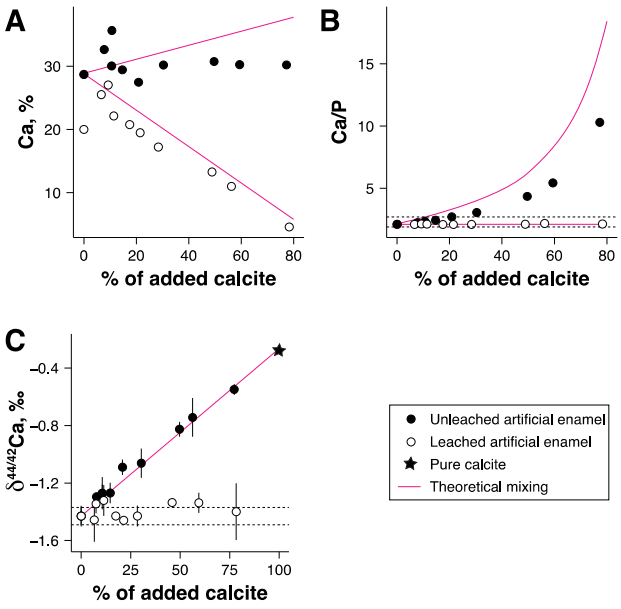

Fig. 2*: Effect of leaching on the Ca concentration (A), Ca/P ratio (B), and the* $\delta^{44/42}$*Ca (C) value of artificial fossil bone material (enamel + SRM-915b). Percentage of added calcite is relative to the initial total mass of the mixture. Error bars are typically < 5% in panel A. Dotted lines in panel B represent the natural range of the Ca/P ratio from 1.9 to 2.7 in biological HAp. Dotted lines in panel C represent the 2 standard deviations of the mean* $\delta^{44/42}$Ca *value of raw material. The* $\delta^{44/42}$*Ca value is reported relative to ICP-Ca Lyon.*

Fossil bone from Camiac (Table S2) shows a Ca/P decrease indicative of efficient removal of additive Ca of calcitic origin (Fig. 3A) along with a consistent decrease (-0.21 ± 0.11, n = 12) of the $\delta^{44/42}$Ca values during the leaching (Fig. 3B), validating the assumption that the added diagenetic Ca from calcite with a higher $\delta^{44/42}$Ca value than bone has been removed accordingly. Fossil enamel unleached and leached samples from Shungura (Table S2) show a Ca/P ratio that remains constant (Fig. 3C) and similar $\delta^{44/42}$Ca values (Fig. 3D), suggesting that non-significant amount of calcite was present in raw samples and that a quantitative fractionation of Ca isotopes occurred during leaching.

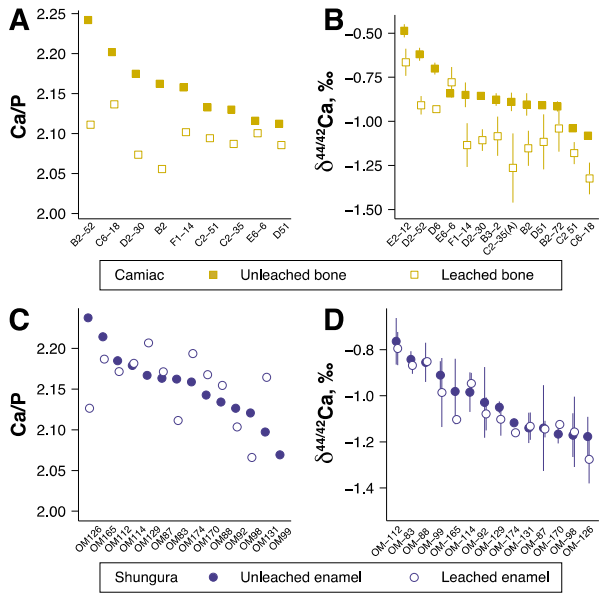

***Fig. 3**: Effect of leaching on the Ca/P ratio and $\delta^{44/42}$Ca value of natural fossil bone from Camiac (A and B) and fossil enamel from Shungura (C and D). The variability of the Ca/P ratio is in the natural range of the Ca/P ratio in biological Hap. The $\delta^{44/42}$Ca value is reported relative to ICP-Ca Lyon.*

Finally, the Devonian bone from Strud (Table S2) show invariable $\delta^{44/42}$Ca values with no preserved trophic information (Fig. 4) despite the leaching procedure. Here, the range of variation of the $\delta^{44/42}$Ca values (0.19‰, n = 25) is much more contracted than at Camiac (0.84‰, n = 26) or Shungura (0.51‰, n = 28). Note that Shungura samples are represented by two taxa of suids only (*Metridiochoerus* sp. and *Notochoerus* sp.), thus are not representative of the possible full trophic variability. The Ca/P range of variation at Strud (2.12 ± 0.07, ± 2SD, n = 25) is in the variability of biological HAp and does not indicate any Ca excess.

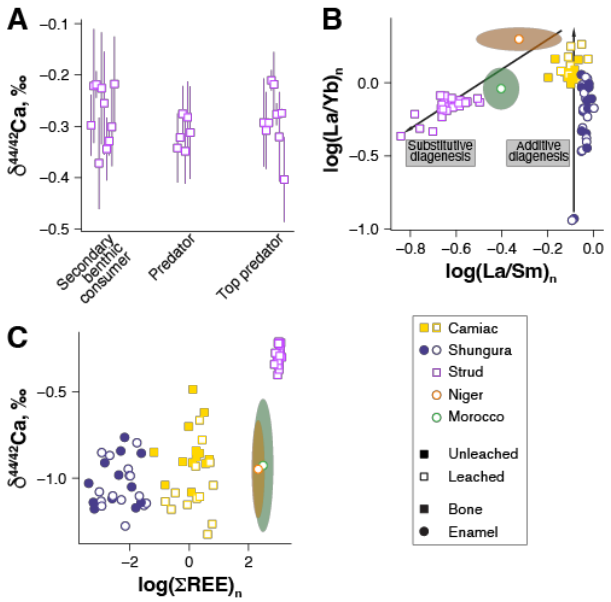

Fig. 4: (A) *$\delta^{44/42}$Ca values of leached bone at Strud. Trophic levels are assessed based on ecomorphological features. (B) $(La/Sm)_n$ vs $(La/Yb)_n$ distribution of fossil samples analyzed in the study. Morocco and Niger samples are from Hassler et al. (2018). REE have been normalized to PAAS. (C) $(\Sigma REE)_n$ vs $\delta^{44/42}$Ca distribution of fossil samples analyzed in the study. Morocco and Niger samples are from Hassler et al. (2018). REE have been normalized to PAAS. The $\delta^{44/42}$Ca value is reported relative to ICP-Ca Lyon.*

Taken together, the results of leaching experiments suggest that Ca isotopes in bone, but not in enamel, are sensitive to an additive-like diagenesis probably because bone porosity is high enough to accommodate significant amount of calcite to modify the original HAp $\delta^{44/42}$Ca value. In case of clear additive-like diagenesis (artificial fossil bone and enamel, Camiac fossil bone) the original HAp $\delta^{44/42}$Ca value is restored by leaching. However, in the case of the Strud fossil bones, the original HAp $\delta^{44/42}$Ca value cannot be restored by leaching as suggested by the absence of trophic pattern. At Strud, fossil bone probably experienced a substitutive-like diagenesis that was sufficiently pervasive to reset original HAp $\delta^{44/42}$Ca values.

4. Discussion

The type of fossil bone and enamel diagenesis, additive or substitutive, can be depicted by the REE pattern, and therefore help to detect whether the Ca isotope composition is potentially reset or not. REE trapping in fossil bone or enamel is a post-mortem phenomenon that occurs through two main processes, namely adsorption and substitution.

The suite of REE differs by ionic radius, middle REE (Sm) having an ionic radius close to that of Ca (~ 100 pm) and thus more liable to incorporate the HAp crystal lattice compared to light (La) or heavy (Yb) REE. The REE pattern can thus typify the nature of diagenetic processes because the relative partitioning among REE will be characteristic of the incorporation process. A quantitative incorporation without relative REE partitioning first occurs during early diagenesis, followed during protracted diagenesis by a non-quantitative adsorption mechanism controlled by surface crystal-chemical properties. Those mechanisms are considered additive in that the REE content increases during diagenesis, constituting an extra burden of trace elements that can be theoretically removed by leaching. While this assumption can be easily accepted concerning fossils that have undergone early diagenesis only, the efficiency of leaching is questionable in case of protracted diagenesis during which recrystallization inevitably occurred (Trueman and Tuross, 2002). Note that Hap recrystallisation, as witnessed by the increase of crystallite size can occur within a few years post-mortem (Trueman et al., 2004), but is linked to the exposure of HAp crystallite surfaces during the breakdown of collagen (Trueman et al., 2008). Finally, a substitution mechanism, which is controlled by bulk crystal-chemical properties, can occur during extensive diagenesis, leading to strong REE partitioning (Reynard et al., 1999), along with progressive transformation of HAp into francolite (Trueman and Tuross, 2002). The effects of this late-stage substitutive-like diagenesis are anticipated to be insensitive to leaching.

As expected, the Late Pleistocene Camiac bone and Early Pleistocene Shungura enamel samples exhibit $(La/Sm)_n$ and $(La/Yb)_n$ ratios characteristic of early diagenesis, supporting the idea that well preserved $\delta^{44/42}Ca$ values (Fig. 4B) can be obtained in leached samples, which is necessary for bone (Fig. 3B) but not for enamel (Fig. 3D) due to the presence of secondary Ca-carbonate in bone but not in enamel. Leaching has no influence on the $(La/Sm)_n$ and $(La/Yb)_n$ ratios for both bone from Camiac and enamel from Shungura (Table S2). The REE pattern at Strud is indicative of a substitutive-like diagenesis (Fig. 4B), and despite leaching, the associated bone $\delta^{44/42}Ca$, which are contracted and invariable among trophic positions, are reset by diagenesis. The picture is however different for fossil enamel. For instance, Cretaceous dinosaur enamel samples from Hassler et al. (2018), which have not been leached, still exhibit highly variable $\delta^{44/42}Ca$ values (from -1.6‰ to -0.4‰) with preserved trophic systematics, despite obvious signs of substitutive-like diagenesis, i.e., hat-shaped REE patterns (Hassler et al., 2018) and low $(La/Sm)_n$ ratios (Fig. 4B). Fossil bone or

277 enamel are open systems and accumulate REE during diagenesis, being through the
278 adsorption and/or the substitution processes. The REE concentration $(\Sigma REE)_n$ thus increases
279 during diagenesis, spanning four orders of magnitude between Shungura enamel samples
280 (0.009 ± 0.020 μg/g, ± 2SD, n = 28, Table S2) and Strud bone samples (1028 ± 724 μg/g, ± 2SD,
281 n = 25, Table S2, Fig. 4C). Dinosaurs enamel samples from Morocco (417 ± 581 μg/g, ± 2SD, n
282 = 23) and from Niger (237 ± 282 μg/g, ± 2SD, n = 49) display high $(\Sigma REE)_n$ concentrations, but
283 still variable $\delta^{44/42}$Ca values despite the absence of leaching.

284 The substitutive-like REE pattern is thus not a good proxy of Ca isotope extended
285 diagenesis in fossil enamel. An explanation is that the enamel one percent of porosity is
286 insufficient to accommodate enough Ca in diagenetic fluids and/or secondary minerals that
287 will further substitute with HAp to significantly modify the isotopic composition of the enamel
288 bulk Ca. This assumption holds providing a realistic $\delta^{44/42}$Ca value of the diagenetic pool (fluid
289 or mineral), which must stand close to the value of river water, i.e., ~0‰ (Heuser et al., 2011;
290 Martin et al., 2017). A simple mass balance calculation indicates that a 1% porosity full of Ca
291 necessitates the diagenetic pool to be ± 4‰ different from the HAp to modify the $\delta^{44/42}$Ca
292 value by ± 0.1‰. In bone, the situation is clearly different because the porosity (~40%) grossly
293 equals the HAp Ca content, so the diagenetic pool can have realistic $\delta^{44/42}$Ca value, i.e., close
294 to that of HAp. Taking all the above results into account, we conclude that Ca isotopes are
295 largely immune to diagenesis in fossil enamel, but not in fossil bone.
296
297 **5. Conclusion**
298 We demonstrate that an addition of a diagenetic phase containing Ca in the form of
299 Ca-carbonate significantly modifies the bulk $\delta^{44/42}$Ca value of artificial fossil bone and enamel,
300 whose initial composition can be restored using leaching. For fossils that have undergone
301 weak diagenesis, this process is reproduced in fossil bone, but not in fossil enamel, which
302 cannot accommodate enough diagenetic Ca in the porosity to modify the bulk $\delta^{44/42}$Ca value.
303 For fossils that have undergone extensive diagenesis, as typified by the REE patterns, leaching
304 is unable to restore the initial bone $\delta^{44/42}$Ca value, while enamel can still contain non-
305 significantly modified $\delta^{44/42}$Ca values, even in the absence of leaching. The diagenetic Ca
306 content that can be added in the porosity during early diagenesis of enamel is too low and is
307 further unable to modify its bulk $\delta^{44/42}$Ca value by substitution. The REE pattern of fossil

enamel is thus not a reliable proxy for extensive diagenetic alteration of Ca isotopes, which remains to be potentially uncovered by crystal-chemical means.

Declaration of competing interest

The authors declare that they have no known competing financial interests or personal relationships that could have appeared to influence the work reported in this paper.

Acknowledgements

Pierre-Jean Dodat received financial supports from the CNRS 80|PRIME program and Research Program of the Nouvelle Aquitaine Region: Isotopes du calcium et anthropobiologie au Paléolithique moyen, convention n° 2019-1R40208. Sébastien Olive received funding from Fonds de la recherche scientifique (FNRS) and the European Union's Horizon 2020 research and innovation programme under the Marie Sklodowska-Curie grant agreement No 101032456-TNT. Kani Bayez, Gaël Clément, Cécilia Cousin, Valentin Fischer, Annelise Folie, Emmanuel Robert, and the Omo Group Research Expedition (OGRE) are thanked for helping with the processing of fossil samples. Sampling authorization was delivered to the OGRE by the Ethiopian Heritage Authority/National Museum of Ethiopia, and a fossil sampling session in Addis Ababa was funded by the project ANR-17-CE27-0002 'DietScratches'. We thank two anonymous reviewers and the Associate Editor Adrian Immenhauser for their in-depth reviews and constructive comments that greatly improve the quality of this article.

Appendix A. Supplementary material

Supplementary figure 1: Mass fractionation in three-isotope space $\delta^{43/42}$Ca vs $\delta^{44/42}$Ca calculated from the measurements of the samples in this study.

Supplementary table 1: Table of results for artificial fossil bone and enamel samples.

Supplementary table 2: Table of results for natural fossil bone and enamel samples.

References

Balter, V., Bocherens, H., Person, A., Labourdette, N., Renard, M., Vandermeersch, B., 2002a. Ecological and physiological variability of Sr/Ca and Ba/Ca in mammals of

West European mid-Würmian food webs. Palaeogeogr., Palaeoclimatol., Palaeoecol. 186, 127–143.

Balter, V., Saliège, J.–F., Bocherens, H., Person, A., 2002b. Evidence of physico–chemical and isotopic modifications in archaeological bones during controlled acid etching. Archaeometry 44, 329–336.

Balter, V., Lécuyer, C., 2004. Determination of Sr and Ba partition coefficients between apatite and water from 5°C to 60°C: a potential new thermometer for aquatic paleoenvironments. Geochim. Cosmochim. Acta 68, 423–432.

Boisserie, J.-R., Guy, F., Delagnes, A., Hlukso, L.J., Bibi, F., Beyene, Y., Guillemot, C., 2008. New palaeoanthropological research in the Plio-Pleistocene Omo Group, Lower Omo Valley, SNNPR (Southern Nations, Nationalities and People Regions), Ethiopia. C. R. Palevol 7, 429–439.

Funston, G.F., dePolo, P.E., Sliwinski, J.T., Dumont, M., Shelley, S.L., Pichevin, L.E., Cayzer, N.J., Wible, J.R., Williamson, T.E., Rae, J.W.B., Brusatte, S.L., 2022. The origin of placental mammal life histories. Nature 610, 107–111.

Hassler, A., Martin, J.E., Amiot, R., Tacail, T., Godet, F.A., Allain, R., Balter, V., 2018. Calcium isotopes offer clues on resource partitioning among Cretaceous predatory dinosaurs. Proc. R. Soc. B 285, 20180197.

Hassler, A., Martin, J.E., Merceron, G., Garel, M., Balter, V., 2021. Calcium isotopic variability of cervid bioapatite and implications for mammalian physiology and diet. Palaeogeogr., Palaeoclimatol., Palaeoecol. 573, 110418.

Hedges, R.E.M., 2002. Bone diagenesis: an overview of processes. Archaeometry 44, 319–328.

Heuser, A., Tütken, T., Gussone, N., Galer, S.J.G., 2011. Calcium isotopes in fossil bones and teeth — Diagenetic versus biogenic origin. Geochim. Cosmochim. Acta 75, 3419–3433.

Hu, Y., Jiang, Q., Liu, F., Guo, L., Zhang, Z., Zhao, L., 2022. Calcium isotope ecology of early Gigantopithecus blacki (∼2 Ma) in South China. Earth Planet. Sci. Lett. 584, 117522.

Jaouen, K., Herrscher, E., Balter, V., 2017. Copper and zinc isotope ratios in human bone and enamel. Am. J. Phys. Anthropol. 162, 491–500.

Joannes-Boyau, R., Adams, J.W., Austin, C., Arora, M., Moffat, I., Herries, A.I.R., Tonge, M.P., Benazzi, S., Evans, A.R., Kullmer, O., Wroe, S., Dosseto, A., Fiorenza, L., 2019. Elemental signatures of Australopithecus africanus teeth reveal seasonal dietary stress. Nature 572, 112–115.

Koch, P.L., Tuross, N., Fogel, M.L., 1997. The Effects of Sample Treatment and Diagenesis on the Isotopic Integrity of Carbonate in Biogenic Hydroxylapatite. J. Archaeol. Sci. 24, 417–429.

376 Kohn, M.J., Moses, R.J., 2013. Trace element diffusivities in bone rule out simple diffusive
377 uptake during fossilization but explain in vivo uptake and release. Proc. Natl. Acad.
378 Sci. USA 110, 419–424.

379 Koutamanis, D., Roberts, G.L., Dosseto, A., 2021. Inter- and intra-individual variability of
380 calcium and strontium isotopes in modern Tasmanian wombats. Palaeogeogr.,
381 Palaeoclimatol., Palaeoecol. 574, 110435.

382 Kral, A.G., Lagos, M., Guagliardo, P., Tütken, T., Geisler, T., 2022. Rapid alteration of cortical
383 bone in fresh- and seawater solutions visualized and quantified from the millimeter
384 down to the atomic scale. Chem. Geol. 609, 121060.

385 Kral, A.G., Ziegler, A., Tütken, T., Geisler, T., 2021. Experimental aqueous alteration of
386 cortical bone microarchitecture analyzed by quantitative micro-computed
387 tomography. Front Earth Sci 9, 609496.

388 Le Houedec, S., Girard, C., Balter, V., 2013. Conodont Sr/Ca and $\delta^{18}O$ record seawater
389 changes at the Frasnian–Famennian boundary. Palaeogeogr., Palaeoclimatol.,
390 Palaeoecol. 376, 114–121.

391 Li, Q., Nava, A., Reynard, L.M., Thirlwall, M., Bondioli, L., Müller, W., 2022. Spatially-
392 Resolved Ca Isotopic and Trace Element Variations in Human Deciduous Teeth
393 Record Diet and Physiological Change. Environ. Archaeol. 27, 474–483.

394 Martin, J.E., Deesri, U., Liard, R., Wattanapituksakul, A., Suteethorn, S., Lauprasert, K., Tong,
395 H., Buffetaut, E., Suteethorn, V., Suan, G., Télouk, P., Balter, V., 2015. Strontium
396 isotopes and the long-term residency of thalattosuchians in the freshwater
397 environment. Paleobiology 42, 143–156.

398 Martin, J.E., Tacail, T., Balter, V., 2017. Non-traditional isotope perspectives in vertebrate
399 palaeobiology. Palaeontology 60, 485–502.

400 Martin, J.E., Tacail, T., Cerling, T.E., Balter, V., 2018. Calcium isotopes in enamel of modern
401 and Plio-Pleistocene East African mammals. Earth Planet. Sci. Lett. 503, 227–235.

402 Martin J.E., Vance, D., Balter, V., 2014. Natural variation of magnesium isotopes in mammal
403 bones and teeth from two South African trophic chains. Geochim. Cosmochim. Acta
404 130, 12–20.

405 McCormack, J., Griffiths, M.L., Kim, S.L., Shimada, K., Karnes, M., Maisch, H., Pederzani, S.,
406 Bourgon, N., Jaouen, K., Becker, M.A., Jöns, N., Sisma-Ventura, G., Straube, N.,
407 Pollerspöck, J., Hublin, J.-J., Eagle, R.A., Tütken, T., 2022. Trophic position of Otodus
408 megalodon and great white sharks through time revealed by zinc isotopes. Nat.
409 Comm. 13, 2980.

410 Nava, A., Lugli, F., Romandini, M., Badino, F., Evans, D., Helbling, A. H., Oxilia, G., Arrighi, S.,
411 Bortolini, E., Delpiano, D., Duches, R., Figus, C., Livraghi, A., Marciani, G., Silvestrini,
412 S., Cipriani, A., Giovanardi, T., Pini, R., Tuniz, C., Bernardini, F., Dori, I., Coppa, A.,

413 Cristiani, E., Dean, C., Bondioli, L., Peresani, M., Müller, W., Benazzi, S., 2020. Early
414 life of Neanderthals. Proc. Natl. Acad. Sci. USA 117, 28719–28726.

415 Nielsen-Marsh, C.M., Hedges, R.E.M., 2000. Patterns of Diagenesis in Bone I: The Effects of
416 Site Environments. J. Archaeol. Sci. 27, 1139–1150.

417 Olive, S., Clément, G., Daeschler, E.B., Dupret, V., 2015. Characterization of the placoderm
418 (Gnathostomata) assemblage from the tetrapod-bearing locality of Strud (Belgium,
419 upper Famennian). Palaeontology 58, 981–1002.

420 Reynard, B., Lécuyer, C., Grandjean, P., 1999. Crystal-chemical controls on rare-earth
421 element concentrations in fossil biogenic apatites and implications for
422 paleoenvironmental reconstructions. Chem. Geol. 155, 233–241.

423 Sillen, A., 1986. Biogenic and Diagenetic Sr/Ca in Plio-Pleistocene Fossils of the Omo
424 Shungura Formation. Paleobiology 12, 311–323.

425 Sillen, A., LeGeros, R., 1991. Solubility profiles of synthetic apatites and of modern and fossil
426 bones. J. Archaeol. Sci. 18, 385–397.

427 Skulan, J., DePaolo D.J., 1999. Calcium isotope fractionation between soft and mineralized
428 tissues as a monitor of calcium use in vertebrates. Proc. Natl. Acad. Sci. USA 96,
429 13709–13713.

430 Suarez, C.A., Kohn, M.J., 2020. Caught in the act: A case study on microscopic scale
431 physicochemical effects of fossilization on stable isotopic composition of bone.
432 Geochim. Cosmochim. Acta 268, 277–295.

433 Tacail, T., Albalat, E., Télouk, P., Balter, V., 2014. A simplified protocol for measurement of
434 Ca isotopes in biological samples. J. Anal. At. Spectrom. 29, 529.

435 Tacail, T., Thivichon-Prince, B., Martin, J.E., Charles, C., Viriot, L., Balter, V., 2017. Assessing
436 human weaning practices with calcium isotopes in tooth enamel. Proc. Natl. Acad.
437 Sci. USA 114, 6268–6273.

438 Trueman, C.N.G., Behrensmeyer, A.K., Tuross, N., Weiner, S., 2004. Mineralogical and
439 compositional changes in bones exposed on soil surfaces in Amboseli National Park,
440 Kenya: diagenetic mechanisms and the role of sediment pore fluids. J. Archaeol. Sci.
441 31, 721–739.

442 Trueman, C.N., Privat, K., Field, J., 2008. Why do crystallinity values fail to predict the extent
443 of diagenetic alteration of bone mineral? Palaeogeogr., Palaeoclimatol., Palaeoecol.
444 266, 160–167.

445 Trueman, C.N., Tuross, N., 2002. Trace Elements in Recent and Fossil Bone Apatite. Rev.
446 Mineral. Geochem. 48, 489–521.

447 Wang, Y., Cerling, T.E., 1994. A model of fossil tooth and bone diagenesis: implications for
448 paleodiet reconstruction from stable isotopes. Palaeogeogr., Palaeoclimatol.,
449 Palaeoecol. 107, 281–289.

450 Wathen, C. A., Isaksson, S., Lidén, K., 2022. On the road again—a review of pretreatment
451 methods for the decontamination of skeletal materials for strontium isotopic and
452 concentration analysis. Archaeol. Anthropol. Sci. 14, 45.

453 Weber, K., Weber, M., Menneken, M., Kral, A. G., Mertz-Kraus, R., Geisler, T., Vogl, J.,
454 Tütken, T., 2021. Diagenetic stability of non-traditional stable isotope systems (Ca,
455 Sr, Mg, Zn) in teeth – An in-vitro alteration experiment of biogenic apatite in
456 isotopically enriched tracer solution. Chem. Geol. 572, 120196.

457